

**SHEAR STRENGTH OF PRESTRESSED AND REINFORCED PRECAST
CONCRETE BEAMS: COMPARISON BETWEEN CODES OF PRACTICE AND
EXPERIMENTAL RESULTS**

Kristof De Wilder, Research Assistant, Dept. of Civil Engineering, Katholieke Universiteit
Leuven, Belgium

Lucie Vandewalle, Full Professor, Dept. of Civil Engineering, Katholieke Universiteit
Leuven, Belgium

ABSTRACT

Shear is one of the topics of fundamental research of reinforced and prestressed concrete members where still disagreement remains amongst researchers. Therefore, codes of practice often use different approaches to the design of concrete structures in shear. This paper presents the results of an experimental program consisting of twelve full scale rectangular precast beams subjected to a four-point bending test up to failure. The investigated parameters were the amount of prestressing force, shear and longitudinal reinforcement and effective depth respectively. A comparison is made between the predicted shear strength according to the American, European and Canadian codes of practice and the experimental results. It was found that all considered sectional procedures underestimated the shear strength with an average predicted-to-experimental shear strength ratio of 0.60 and an average coefficient of variation (COV) of 26%. An alternative design procedure, based on the arching effect, is proposed with an average shear strength ratio of 0.94 and a COV of 4%.

Keywords: Shear Strength, Prestressed Concrete, Design

INTRODUCTION

For more than a century, shear is one of a few areas of fundamental research of concrete structures where disagreement remains amongst researchers. Since the early days of concrete construction, engineers have sought for models that accurately describe and determine the resistance of members in shear. In his publication *Die Bauweise Hennebique* of 1899, Ritter presented steel strips as shear reinforcement and the calculation of the required amount was based on a truss model. Morsch adopted the idea of Ritter and proposed a similar truss model for torsion. This methodology is the well-known Ritter-Morsch truss analogy and is still the basis for many codes of practice today. Over the years, shear remained a field of much interest and from 1950 on research effort has been growing substantially. Due to the many factors that influence the shear capacity, shear is a very complex phenomenon. Many of the proposed analytical models are therefore (semi-) empirical and not suitable for the whole spectrum of structural concrete members. In the last three decades, focus has shifted to theoretical analytical models, thus decoupling themselves as much as possible from empirical dependencies. Some of these models are mature enough to be incorporated into codes of practice. This paper presents a comparison between test results and predicted shear strengths based on the American (ACI 318-08), the European (EN 1992-1-1:2005) and the Canadian (CSA A.23-3.04) code of practice respectively.

THEORETICAL CONSIDERATIONS AND CODE PROVISIONS

In order to fully understand the current code provisions for shear in reinforced and prestressed concrete structural members, it is necessary to consider the development of shear research during the last century. In the early 1900s, truss models were used as conceptual tools in the analysis and design of reinforced concrete beams. Ritter¹ postulated in 1899 that, after the web of a beam cracks due to diagonal tension stresses, the internal bearing system can be represented as a parallel chord truss with compressive diagonals inclined at approximately 45 degrees. These diagonal compressive stresses push apart the top and bottom faces of the beam while shear reinforcement is required to pull these faces back together. The shear capacity is reached when the stirrups yield and will correspond to a shear stress of

$$v = \frac{A_v f_y}{b_w s} = \rho_v f_y \quad (1)$$

Morsch^{2,3} adopted the idea of Ritter and introduced the use of truss models for torsion. Several researchers^{4,5} pointed out that the use of this truss model gave conservative results. Based on numerous test results, two different concepts were introduced to ensure economy in the practical design: (1) the so-called ‘concrete contribution’ V_c and later (2) a variable compressive strut inclination.

The concept of concrete contribution refers to the ability of concrete structures without shear reinforcement to carry a certain amount of shear force. This concrete contribution is usually

attributed to one or more of the following five mechanisms⁶: (1) shear stresses in the uncracked concrete, (2) interface shear transfer, often referred to as crack friction or aggregate interlock, (3) dowel action of the flexural reinforcement, (4) residual tensile stresses transmitted directly across cracks and (5) arch action. Different researchers assign a different relative importance to these aforementioned mechanisms, resulting in various (semi)-empirical expressions for the concrete contribution. Therefore, the expressions found in codes of practice for the concrete contribution differ greatly. The 45 degree truss model with an additional concrete contribution term is often referred to as the standard method.

From the 1960s to the 1980s, the pioneering work of Ritter and Mörsh received new impetus. Based on an extensive amount of test results, researchers⁷⁻¹⁰ proposed a truss with inclined compressive struts with angles which are allowed to differ from 45 degrees within certain limits suggested on the basis of plasticity. This method is often referred to as the variable angle truss method. It does not consider a concrete contribution but due to the existence of aggregate interlock and dowel forces at the crack faces, a lower inclination of the compressive strut is possible and thus further mobilization of the stirrup reinforcement. The shear stress at failure in its more general form is thus given by

$$v = \frac{A_v f_y}{b_w s} \cot \theta = \rho_v f_y \cot \theta \quad (2)$$

where θ is the angle of inclination of the compressive struts with respect to the horizontal axis. Members with an applied axial compressive load usually exhibit a crack pattern with lower inclinations than 45 degrees and thus require less shear reinforcement.

A combination of the variable angle strut inclination and a concrete contribution has also been proposed and has been referred to as the modified truss model approach^{11,12}. In this approach, in addition to a variable angle of inclination of the compressive struts, the concrete contribution diminishes for nonprestressed beams with the level of shear stress. For prestressed beams, the concrete contribution does not vary with the level of shear stress and is a function of the level of prestress in the extreme tension fiber.

ACI 318-08

The shear design expressions found in the current American code of practice¹³ are based on the aforementioned 45 degree truss model with an experimentally obtained concrete contribution term. An overview of the history of the shear provisions can be found in the report of the Joint ACI-ASCE Committee 445⁶. The approach assumes that flexure and shear can be handled separately for the worst case of bending moment and shear force. The interaction between flexure and shear, i.e. increase of tensile force in the flexural reinforcement due to inclined cracking, is addressed by detailing rules for flexural reinforcement cutoff points. In addition, specific checks on the level of concrete stresses in the member are introduced to ensure ductile behavior and control of diagonal crack widths at service load levels. Equations (3)-(13) give an overview of the current ACI design procedure where SI-units should be used (note: 1 MPa = 145 psi; 25.4 mm = 1 in.; 1 kip = 4448 N = 1 kip).

$$V_n = V_c + V_s \quad (3)$$

$$V_s = \frac{A_v f_{yt} (\sin \alpha + \cos \alpha) d}{s} \quad (4)$$

$$V_c = \text{concrete contribution} \quad (5)$$

For nonprestressed beams

$$0.17\lambda\sqrt{f_c'}b_wd \quad (6)$$

where λ is a factor to account for the use of lightweight concrete. For normal weight concrete this factor is equal to 1. When a more detailed calculation is made, the concrete contribution is given by

$$\left(0.16\lambda\sqrt{f_c'} + 17\rho_w \frac{V_u d}{M_u} \right) b_w d \leq 0.29\lambda\sqrt{f_c'}b_wd \quad (7)$$

For prestressed beams

$$\left(0.05\lambda\sqrt{f_c'} + 4.8 \frac{V_u d_p}{M_u} \right) b_w d \quad (8)$$

but

$$0.17\lambda\sqrt{f_c'}b_wd \leq V_c \leq 0.42\lambda\sqrt{f_c'}b_wd \quad (9)$$

or the lesser of V_{ci} and V_{cw}

$$V_{ci} = 0.05\lambda\sqrt{f_c'}b_wd_p + V_d + \frac{V_i M_{cre}}{M_{max}} \leq 0.17\lambda\sqrt{f_c'}b_wd \quad (10)$$

$$V_{cw} = (0.29\lambda\sqrt{f_c'} + 0.3f_{pc})b_wd_p + V_p \quad (11)$$

For axial compression and shear

$$0.17 \left(1 + \frac{N_u}{14A_g} \right) \lambda\sqrt{f_c'}b_wd \quad (12)$$

For axial tension and shear

$$0.17 \left(1 + \frac{0.29N_u}{A_g} \right) \lambda\sqrt{f_c'}b_wd \quad (13)$$

It is clear that the shear provisions used in the American code of practice are semi-empirical expressions. The primary shortcomings of ACI 318-08 are the many empirical equations and rules for special cases, and particularly the lack of a clear model that can be extrapolated to cases not directly covered.

EUROCODE 2

Until recently, one could choose when dealing with shear design between the standard method (45 degree truss model with concrete contribution term) and the variable angle truss method in Eurocode 2 (EC2). In the latest edition of EC2¹⁴ however, only the variable angle truss method is still valid and thus applicable. The approach uses three different shear strengths: (1) $V_{Rd,c}$, (2) $V_{Rd,max}$ and (3) $V_{Rd,s}$. The shear strength of members without shear reinforcement is given by Eq. (14).

$$V_{Rd} = V_{Rd,c} \quad (14)$$

From Eq. (14) it can be seen that the total shear strength equals the concrete contribution defined in Eq. (15).

$$V_{Rd,c} = \left(C_{Rd,c} k (100 \rho_l f_{ck})^{\frac{1}{3}} + k_1 \sigma_{cp} \right) b_w d \geq (v_{\min} + k_1 \sigma_{cp}) b_w d \quad (15)$$

where $C_{Rd,c}$ equals $0.18/\gamma_c$ and k_1 can be taken equal to 0.15. Eq. (15) is experimentally derived and incorporates the main shear carrying mechanisms of beams without shear reinforcement as discussed earlier. The shear capacity of members with shear reinforcement is completely determined by the amount of shear reinforcement.

$$V_{Rd} = \frac{A_{sw}}{s} z f_{ywd} \cot \theta \quad (16)$$

The limits for the angle of inclination can be found in national application documents. Specifically for the Belgian context¹⁵, the limits are given by

$$1 \leq \cot \theta \leq \cot \theta_{\max} = \left(2 + \frac{k_1 \sigma_{cp} b_w d s}{A_{sw} z f_{ywd}} \right) \leq 3 \quad (17)$$

From Eq. (17) it can be seen that the angle of inclination depends on the level of applied axial force by means of σ_{cp} . When an axial compressive force is applied (e.g. prestressing force) the angle becomes lower, whereas the application of an axial tensile force will result in higher angles of inclination. Lower angles of inclination result in less shear reinforcement according to Eq. (16) which is expected for prestressed members. To prevent the concrete struts from crushing, the maximum allowable shear force is given by

$$V_{Rd,max} = \frac{\alpha_{cw} b_w z v_1 f_{cd}}{\cot \theta + \tan \theta} \quad (18)$$

In Eq. (18) v_l is a term to account for the compressive strength reduction of cracked concrete and can be taken as 0.6 for normal strength concrete (NSC).

CANADIAN CODE

The shear design provisions found in the Canadian code of practice can be traced back to a rational theoretical model that determines the angle of inclination by considering the deformation of the longitudinal and transverse reinforcement and the diagonally stressed concrete. Such procedures are known as compressive field approaches. Kupfer⁷ and Baumann¹⁶ presented approaches in the 1960s and 1970s for determining the angle of inclination assuming that concrete and reinforcement behave linear elastically. When studying ultimate strengths however, it is necessary to also address the nonlinear behavior of concrete. Methods for determining the angle θ for the full loading range were determined by Collins¹⁷ for members in shear. This procedure is known as the Compression Field Theory (CFT). The CFT considers three major sets of equations: (1) equilibrium equations, (2) compatibility equations and (3) stress-strain relationships. Fig. 1 summarizes the basic relationships of the CFT. When a shear stress v is applied to a reinforced cracked concrete panel, it causes tensile stresses in the longitudinal reinforcement f_{sx} and the transverse reinforcement f_{sy} and concrete compressive stresses f_2 inclined at an angle θ . Equilibrium relationships in combination with Mohr's circle for stresses (Fig 1(a) and Fig. 1(b)) are given by

$$\rho_y f_{sy} = f_{cy} = v \tan \theta \quad (19)$$

$$\rho_x f_{sx} = f_{cx} = v \cot \theta \quad (20)$$

$$f_2 = v(\tan \theta + \cot \theta) \quad (21)$$

where ρ_x and ρ_y are the longitudinal and transverse reinforcement ratios respectively. Under the applied stresses, the concrete compressive strut will shorten by a strain equal to ε_2 , the longitudinal reinforcement will elongate by a strain ε_x and the transverse reinforcement by a strain ε_y . Using Mohr's circle for strain, the direction of the principal compressive strain and the value of the principal tensile strain are then given by

$$\tan^2 \theta = \frac{\varepsilon_x + \varepsilon_2}{\varepsilon_y + \varepsilon_2} \quad (22)$$

$$\varepsilon_1 = \varepsilon_x + (\varepsilon_x + \varepsilon_2) \cot^2 \theta \quad (23)$$

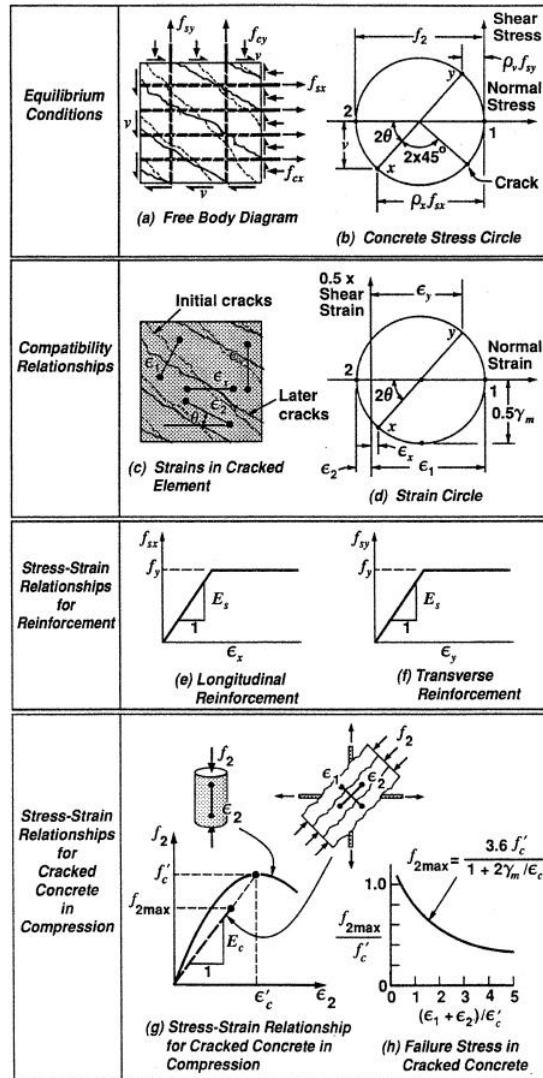


Fig. 1 Compression Field Theory⁶

Before these equations can be used, stress-strain relationships need to be defined for both the concrete in compression and the reinforcing steel. It is assumed that the reinforcement strains are related to the reinforcement stresses according to the simple bilinear diagram shown in Fig. 1(e) and (f). Thus, after the strain in the reinforcement reaches the yield strain, the stress in the reinforcing steel will remain constant with increasing strain. Concrete in compression is somewhat more difficult to describe. Based on test results, Collins stated that the behavior of diagonally cracked concrete differs greatly from the usual compressive behavior of a standard cylinder. It was found that the principal compressive stress f_2 is not only dependent on the principal compressive strain ϵ_2 but also on the perpendicular principal tensile strain ϵ_1 . When concrete is diagonally cracked, compressive stresses need to be transferred by aggregate interlock. Increasing principal tensile strain, and thus increasing crack width, will result in lower aggregate interlock stresses and thus a lower compressive strength. The relationship proposed is depicted in Fig. 1(g) and (h). Cracked concrete is thus considered as

an orthotropic material with smeared cracks. For a reinforced concrete panel subjected to only shear stresses, Eq. (19)-(23) together with the described stress-strain relationships will give the internal stresses, direction of principal compressive stresses and thus the failure mode. Note that beams are usually subjected to a varying bending moment along the length of the beam and a corresponding shear force. The bending moment increases ε_x and thus lowers the shear capacity.

The Modified Compression Field Theory (MCFT)¹⁸ proposed by Vecchio and Collins, is a further development of the CFT. It accounts for the influence of tensile stresses in the cracked concrete. It is also recognized that the concrete and reinforcement stresses vary from point to point with high reinforcement and no concrete stresses at crack locations. Compatibility relationships and equilibrium equations are therefore defined in terms of average strains and average stresses respectively, averaged out over a base length that is longer than the crack spacing. Fig. 2 depicts the basic relationships of the MCFT. Equilibrium equations in terms of average stresses in combination with Mohr's circle for average stresses and taking into account tensile stresses in the cracked concrete are given by

$$\rho_y f_{sy} = f_{cy} = v \tan \theta - f_1 \quad (24)$$

$$\rho_x f_{sx} = f_{cx} = v \cot \theta - f_1 \quad (25)$$

$$f_2 = v(\tan \theta + \cot \theta) - f_1 \quad (26)$$

In order to use Eq. (24)-(26), the stress-strain relationship of concrete in tension needs to be defined. Vecchio and Collins propose a linear elastic behavior until the strain reaches the cracking strain. From this point on, tensile stresses will diminish with increasing strain in order to model the tension stiffening effect as shown in Fig. 2(e). Equilibrium equations (24)-(26), together with the earlier discussed strain compatibility relationships (in terms of average strains) and the stress-strain relationships for reinforcing steel and concrete (compressive and tensile), will enable to determine the angle of compressive stresses, average stresses and average strains.

Failure of the reinforced concrete element may be governed not by average stresses, but rather by local stresses that occur at a crack. Therefore, an additional check must be performed at the crack face. In checking the conditions at a crack, the actual complex crack pattern is idealized as a series of parallel cracks, all occurring at an angle θ to the horizontal and having a space s_θ between them. From Fig. 2(c), the reinforcement stresses at a crack can be determined as

$$\rho_y f_{sycr} = v \tan \theta - v_{ci} \tan \theta \quad (27)$$

$$\rho_x f_{sxcr} = v \cot \theta - v_{ci} \cot \theta \quad (28)$$

where v_{ci} is the shear stress on the crack face due to aggregate interlock. The maximum possible value of v_{ci} is proposed by Collins and Bhide¹⁹ based on the work of Walraven²⁰ and

is taken to be related to the crack width w and the maximum aggregate size a_g . It can be expressed as

$$v_{ci} \leq \frac{0.18\sqrt{f_c'}}{0.3 + \frac{24w}{a_g + 16}} \quad (29)$$

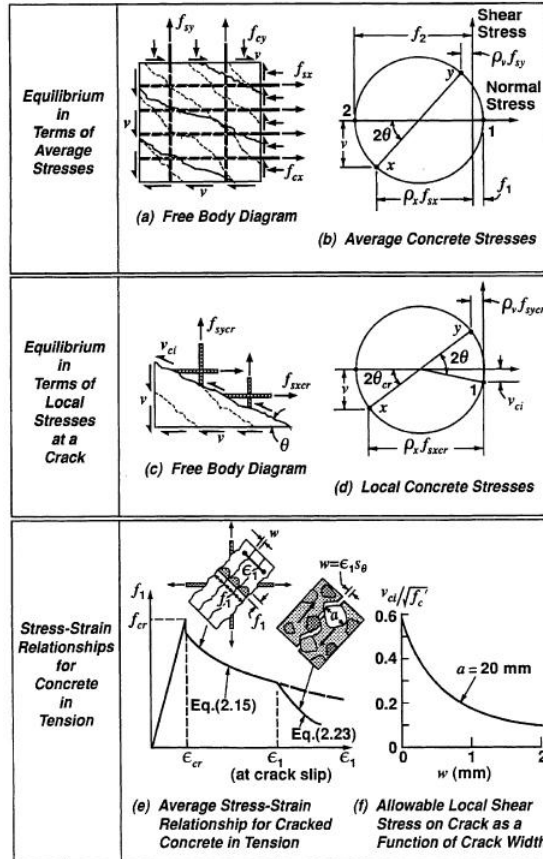


Fig. 2 Modified Compression Field Theory⁶

The crack width w is taken as the crack spacing times the principal tensile strain ϵ_t . By limiting the maximum value for v_{ci} , the model takes into account the possibility of failing of the aggregate interlock mechanism. Eq. (27) and (28) can be satisfied without the term v_{ci} if the reinforcement does not yield. From yielding on, shear stresses on the crack face are needed so that equilibrium remains but they cannot exceed the maximum value given in Eq. (29).

To determine the full load-deformation response of a concrete beam, the member must be represented as a two-dimensional array of concrete panels. Solving this system usually requires the use of a non-linear finite element computer program^{21,22}. If one is only interested

in the shear strength of a beam cross-section, then the web of the beam can be represented by just one biaxial element located at mid-depth. It is assumed that, at failure, the stirrups will yield and that the shear stress in the web can be determined by dividing the actual shear force by the effective shear area $b_w d$. Eq. (27) can be rearranged to give

$$v = v_{ci} + \rho_y f_y \cot \theta \quad (30)$$

with f_y the yield stress of the reinforcement. In a similar way, Eq. (24) can be rearranged as

$$v = f_1 \cot \theta + \rho f_y \cot \theta \quad (31)$$

Both these equations can be written in following form

$$v_r = v_c + v_s \quad (32)$$

where v_r is the shear strength and consists of a concrete and shear reinforcement component. A more general form in terms of forces is given by

$$V_r = V_c + V_s + V_p \leq V_{r,\max} \quad (33)$$

$$V_r = f_1 b_w d_v \cot \theta + \frac{A_v f_y}{s} d_v \cot \theta + V_p \leq V_{r,\max} \quad (34)$$

$$V_r = \beta \sqrt{f_c} b_w d_v \cot \theta + \frac{A_v f_y}{s} d_v \cot \theta + V_p \leq V_{r,\max} \quad (35)$$

Both β and θ depend on the amount of longitudinal strain in the web. The larger this longitudinal strain becomes, the smaller the shear stress required to fail the web, as discussed earlier. It is conservative to use the highest possible longitudinal strain found in the longitudinal reinforcement. It is proposed to use the strain at mid-depth, given by Eq. (36).

$$\varepsilon_x = \frac{\frac{M_u}{d_v} + 0.5N_u + 0.5V_u \cot \theta - A_{ps} f_{p0}}{2(E_s A_s + E_p A_{ps})} \quad (36)$$

The strain in Eq. (36) shall not be taken greater than 0.002. These aforementioned expressions can be found in the Canadian code of practice CAN CSA A.23.3-04²³. Expressions for β and θ are given in Eq. (37) and (38)

$$\beta = \frac{0.4}{1 + 1500\varepsilon_x} \cdot \frac{1300}{1000 + s_{xe}} \quad (37)$$

$$\theta = (29^\circ + 7000\varepsilon_x) \quad (38)$$

where s_{xe} is the equivalent crack spacing parameter and equal to $35s_x/(a_g+16)$.

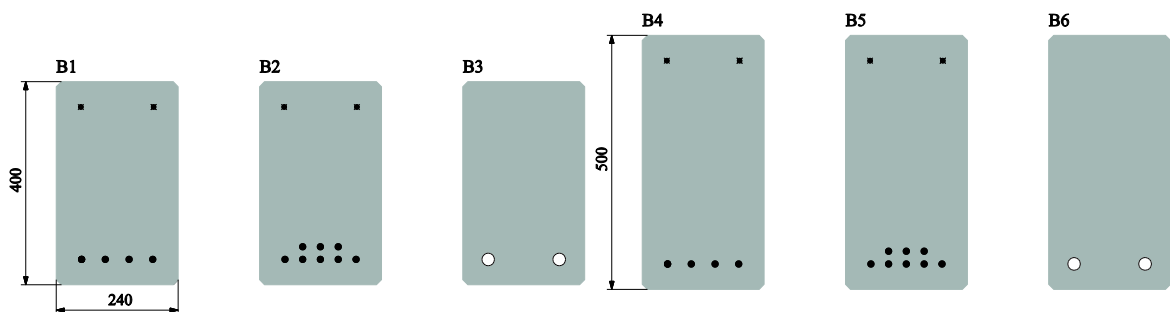
EXPERIMENTAL INVESTIGATION

SPECIMEN DESIGN

The purpose of the experimental campaign was to evaluate the shear strength of precast concrete beams and consisted of 12 full-scale rectangular specimens. The main investigated parameters were the amount of prestressing force, the amount of longitudinal mild steel and shear reinforcement and the effective depth respectively. Table 1 shows an overview of the experimental program. All specimens had a total length of 6000 mm (19.7 ft.). Fig. 3 depicts the cross section details.

Table 1 Specimen details

Specimen	width mm (in.)	height mm (in.)	Prestressed strands		Longitudinal reinforcement Area mm ² (in. ²)	Shear reinforcement	
			12.5 mm (1/2 in.)	9.3 mm (3/8 in.)		ϕ mm (in.)	s mm (in.)
B1	240 (9.5)	400 (15.8)	4	2	0	0	0
B2	240 (9.5)	400 (15.8)	8	2	0	0	0
B3	240 (9.5)	400 (15.8)	0	0	982 (1.5)	0	0
B4	240 (9.5)	500 (19.7)	4	2	0	0	0
B5	240 (9.5)	500 (19.7)	8	2	0	0	0
B6	240 (9.5)	500 (19.7)	0	0	982 (1.5)	0	0
B7	240 (9.5)	500 (19.7)	8	2	0	6 (0.2)	300 (11.8)
B8	240 (9.5)	600 (23.6)	4	2	982 (1.5)	0	0
B9	240 (9.5)	600 (23.6)	8	2	0	0	0
B10	240 (9.5)	500 (19.7)	4	2	982 (1.5)	0	0
B11	240 (9.5)	600 (23.6)	4	2	982 (1.5)	6 (0.2)	300 (11.8)
B12	240 (9.5)	600 (23.6)	8	2	0	6 (0.2)	300 (11.8)



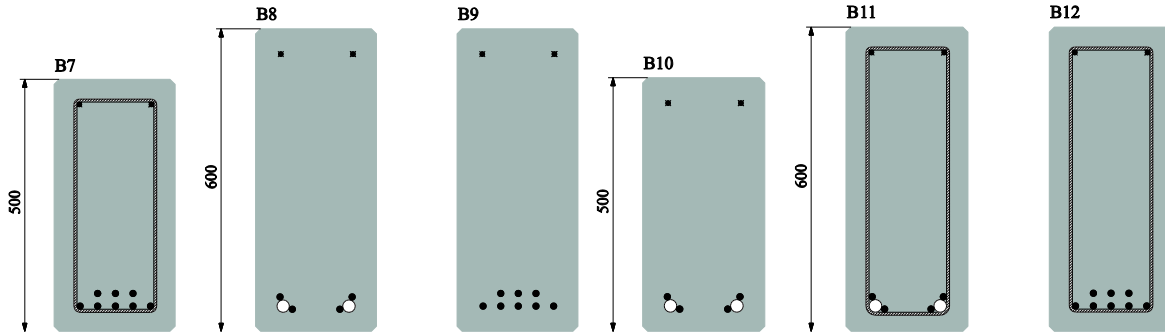


Fig. 3 Cross section details

MATERIALS

Prestressed reinforcement consisted of low-relaxation seven-wire strands with a nominal diameter of 12.5 mm (1/2 in.) or 9.3 mm (3/8 in.). The ultimate tensile strength was given by the manufacturer and is equal to 1930 MPa (280 ksi). The conventional longitudinal reinforcement consisted of hot rolled bars with a diameter of 25 mm (0.98 in.) and an ultimate tensile strength of approximately 600 MPa (87 ksi). Concrete was factory-made and was designed to have a characteristic cylinder strength of 50 MPa (7250 psi). Cement was specified as CEM I 52.5 R whereas the coarse aggregate consisted of 12 mm (0.5 in.) maximum-size lime stone gravel. A high-range water reducer was also provided. Table 2 lists the mix details. The concrete mixtures had a water-cement ratio of 0.42.

Table 2 Concrete batch weights

Material	amount
Cement CEM I 52.5 R, kg/m ³ (lb/yd ³)	397 (669)
Lime stone gravel 2/12, kg/m ³ (lb/yd ³)	1095 (1846)
Sand 0/2, kg/m ³ (lb/yd ³)	663 (1118)
Water, kg/m ³ (lb/yd ³)	168 (283)
Filler, kg/m ³ (lb/yd ³)	168 (283)
High-range water reducer l/m ³ (oz/yd ³)	7.1 (185)

CASTING AND CURING

Concrete mixtures were made in volumes of 2 m³ (2.6 yd³). Every beam consisted of just one mixture. Per mixture three prisms were cast to determine the flexural tensile strength, $f_{ct,fl}$. Per beam, three cubes with sides of 150 mm (9.8 in.) were cast to determine the compression strength, $f_{cm,cube}$. The mechanical properties of the concrete are denoted in Table 3. All beams were cast into steel formwork and compacted with an internal vibrator. After setting, the beams were covered with plastic sheeting. The steel formwork was removed in less than 24 hours after casting. The day after casting, demountable mechanical strain gauge points (DEMEC-points) were glued to the concrete surface in the zones where shear failure could occur. These points had a spacing of 100 mm (4 in.) or 200 mm (8 in.).

STRESSING PROCEDURE

The prestressing strands were tensioned the day prior to casting. The strand force was measured using a pressure transducer installed on the hydraulic jack. Every strand was given an initial prestrain of 7.5 mS or 1488 MPa (216 ksi). The day after casting, with the formwork removed and the DEMEC-points attached, a first reference measurement was performed. After cutting of all the strands, a second strain measurement followed to determine the immediate losses due to the release of the prestressing force. Beams were tested at an age of 30-56 days. The effective prestress at the day of testing was calculated taking into account the initial prestress loss and additional losses due to the combined working of creep, shrinkage and relaxation. The effective prestress force F_e is also listed in Table 3.

TEST SETUP AND PROCEDURE

The test setup consisted of a simply supported beam with two concentrated loads Q applied at a distance a from the support, as depicted in Fig. 4. The distance a is 1200 mm (3.8 ft.) for beams with a height of 400 (16 in.) or 500 mm (20 in.) and is 1800 mm (5.8 ft.) for beams with a height of 600 mm (24 in.). This results in a shear span to depth ratio range between 2.6 and 3.6. Every specimen was tested with one meter (3.2 ft.) cantilever. This has two reasons; the (1) first is to prevent failure due to the loss of anchorage. The (2) second reason is to study shear in a zone outside the length needed for the prestressing force to gradually develop over the total depth of the member.

Table 3 Mechanical properties of concrete and effective prestress force

Specimen	$f_{cm,cube}$ MPa (psi)	$f_{ct,fl}$ MPa (psi)	F_e kN (kip)
B1	64 (9280)	7 (1015)	645 (145)
B2	72 (10440)	7 (1015)	1030 (232)
B3	70 (10150)	10 (1450)	0 (0)
B4	69 (10000)	7 (1015)	655 (147)
B5	68 (9860)	7 (1015)	1057 (238)
B6	65 (9430)	10 (1450)	0 (0)
B7	65 (9430)	6 (870)	1063 (239)
B8	70 (10150)	9 (1305)	667 (150)
B9	63 (9140)	6 (870)	1075 (238)

B10	71 (10300)	9 (1305)	662 (149)
B11	63 (9140)	6 (870)	665 (150)
B12	57 (8270)	7 (1015)	1070 (241)

The force was applied by a hydraulic press with a contact surface area of 800x800 mm² (32x32 in.²). A steel profile lying on two rollers clamped between steel bearing plates, transforms the force from the press to two point loads Q . To avoid stress concentrations, a layer of plaster is placed between the concrete top surface and the steel bearing plates. The failure load $Q_{u,pred}$ was calculated with all safety factors equal to 1 and loads were applied at 50%, 75%, 90% and 100% of $Q_{u,pred}$. Higher loads were applied in increments of 5% or 10%. Per loading stage, deformations on the concrete side surfaces were measured with DEMEC, the midspan deflection was measured with a deformation gauge and the crack pattern was photographed. The ultimate force at failure can be read from the display of the hydraulic press.

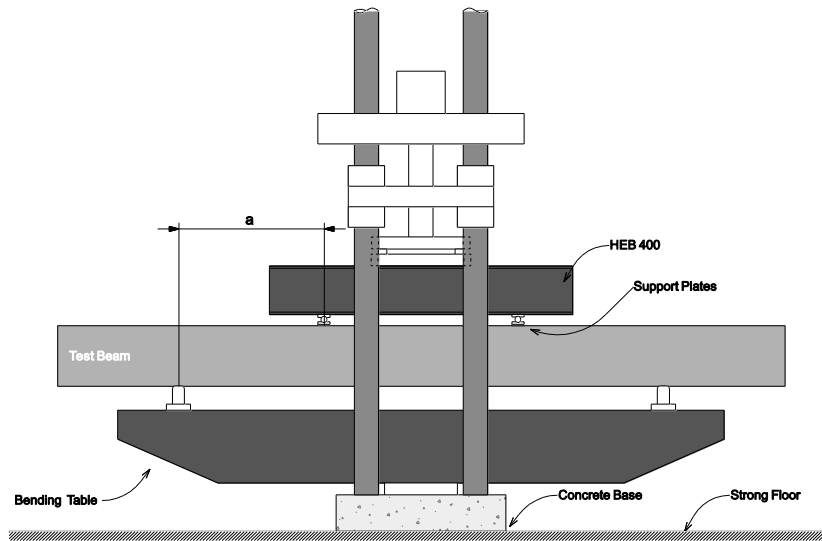


Fig. 4 Test setup

TEST RESULTS AND DISCUSSION

Table 4 lists the failure load, $Q_{u,test}$, and mode together with the predicted shear strengths according to the Canadian, European and American codes of practice. The load necessary to obtain the beam bending capacity is also listed and denoted as $Q_{u,flex}$. It must be noted that specimen B3 is not listed in the aforementioned table. During the testing of B3, a sudden stage of unloading occurred. When reapplying the load, the specimen suddenly failed without exhibiting a profound cracking pattern. In order to avoid false conclusions, the specimen will

be no longer considered. All predicted values for the failure load $Q_{u,pred}$ were obtained by using safety factors equal to 1, average compressive strengths instead of characteristic values and the yield strength for steel. Even with all safety removed from the equations, it can be seen from Table 4 that the considered codes of practice severely underestimate the shear strength, and thus the failure load. Only for beam B11 does the Canadian code predict a slightly higher strength than actually measured. The average ratio of predicted-to-test failure load ratio is 69% for the Canadian code and 56% for EC2 and ACI318-08. This leads to highly conservative predictions for the considered test beams when the usual safety factors are applied. It can be seen that the variation of the predicted-to-test failure load ratio of ACI 318-08, expressed as the coefficient of variation (COV), is the smallest: 17%. The Canadian code shows a normalized dispersion of 26% whereas EC2 has a COV of 34%.

Table 4 Experimental and predicted strengths

Specimen	$Q_{u,test}$ kN (kip)	CSA A.23.3-04		EN 1992-1-1:2005		ACI 318-08		$Q_{u,flex}$ kN (kip)	Failure mode
		$Q_{u,pred}$ kN (kip)	$\frac{Q_{u,pred}}{Q_{u,test}}$	$Q_{u,pred}$ kN (kip)	$\frac{Q_{u,pred}}{Q_{u,test}}$	$Q_{u,pred}$ kN (kip)	$\frac{Q_{u,pred}}{Q_{u,test}}$		
B1	196 (44)	147 (33)	0.75	162 (36)	0.82	129 (29)	0.66	172 (39)	B
B2	325 (73)	221 (50)	0.68	224 (50)	0.69	182 (41)	0.56	325 (73)	B
B4	259 (58)	178 (40)	0.69	175 (39)	0.67	173 (39)	0.67	226 (51)	B
B5	455 (102)	278 (63)	0.61	245 (55)	0.54	251 (56)	0.55	433 (97)	B
B6	222 (50)	103 (23)	0.47	119 (27)	0.54	144 (32)	0.65	173 (39)	A
B7	446 (100)	326 (73)	0.73	102 (23)	0.23	253 (57)	0.57	431 (97)	B
B8	318 (72)	189 (43)	0.59	237 (53)	0.74	155 (35)	0.49	317 (71)	B
B9	381 (86)	250 (56)	0.66	262 (59)	0.69	232 (52)	0.61	346 (78)	B
B10	413 (93)	178 (40)	0.43	221 (50)	0.54	162 (36)	0.39	382 (86)	A
B11	370 (83)	383 (86)	1.03	129 (29)	0.35	155 (35)	0.42	315 (71)	B
B12	385 (87)	363 (82)	0.94	126 (28)	0.33	231 (52)	0.60	355 (80)	B
		μ	0.69		0.56		0.56		
		COV	26%		34%		17%		

B = Bending; A = Anchorage Failure

Table 4 also denotes the failure modes. All specimens were designed to fail in shear. However, in this experimental program no specimen failed due to shear. Two beams (B6 and B10) failed due to the loss of anchorage and the remaining 10 specimens all exhibited failure due to bending. All experimental failure loads are higher or equal to the flexural failure load $Q_{u,flex}$.

The influence of all other parameters is investigated for each code of practice separately and is depicted in Fig. 5(a)-(i). To assess the influence of the amount of shear reinforcement, the sets (B5, B7), (B9, B12) and (B8, B11) can be considered while other parameters are kept constant. The influence of the shear span to depth ratio can be investigated by considering (B1, B4), (B2, B5, B9), (B7, B12) and (B8, B10). To analyze the impact of the amount of prestressing on the shear strength predictions, beams (B1, B2) and (B4, B5, B6) will be investigated.

CAN CSA A.23.3-04

From Fig. 5(a) it seems that an increase of shear reinforcement, leads to better predictions of the ultimate shear strength. The strength of members without shear reinforcement is strongly underestimated whereas the average ratio of predicted to experimental shear strength of the equivalent beams with shear reinforcement equals approximately 0.90. Fig. 5(b) shows the trend that members with lower shear span to depth ratios will result in lower shear strength predictions. The explanation could be that arching action becomes more important in members with shear span to depth ratios below 2.5. This mechanism is not accounted for in the shear strength provisions of the Canadian code of practice. The influence of the amount of prestressing is not clear from Fig. 5(c). The overall shear strength capacity relative to the experimentally measured failure load seems to increase (B6 –B4) and decrease (B4 – B5 and B1 – B2) with increasing amount of prestressing force.

ACI 318-08

There is no general influence of the amount of shear reinforcement on the shear strength predictions as shown in Fig. 5(d). Only when comparing beams B8 and B11 a slight decrease in predicted-over-experimental failure load is found with increasing amount of shear reinforcement. Fig. 5(e) also seems to show that the shear span to depth ratio does not have a great influence on the ultimate strength prediction. A slight decrease in predicted-over-experimental failure load is observed with decreasing shear span to depth ratio for beams B8 and B10 (both 600 mm (23.6 in.) high). However, this trend is not observed for beams (B2, B5, B9), (B1, B4) or (B7, B12). When examining the influence of the amount of prestressing on the failure load, a pattern similar to the one found in Fig. 5(c) is observed in Fig. 5(f). A slight increase (B6-B4) and decrease (B4-B5 and B1-B2) is found with increasing amount of prestressing.

EN 1992-1-1:2004

It is clear from Fig. 5(g) that the failure load of beams with shear reinforcement is very poorly predicted with respect to beams without shear reinforcement. As already mentioned, the shear capacity of beams with shear reinforcement is completely determined by the amount of stirrups. Beams B7, B11 and B12 were equipped with minimum shear reinforcement hence the low predicted shear strength. Fig. 5(h) seems to indicate that decreasing values for the shear span to depth ratio result in decreasing predicted-over-experimental values. Arching action might also here be the reason for this discrepancy. In Fig. 5(i) again the same pattern is detected: increasing (B6-B4) and decreasing (B4-B5 and B1-B2) predicted-over-experimental failure load ratios with increasing amount of prestressing.

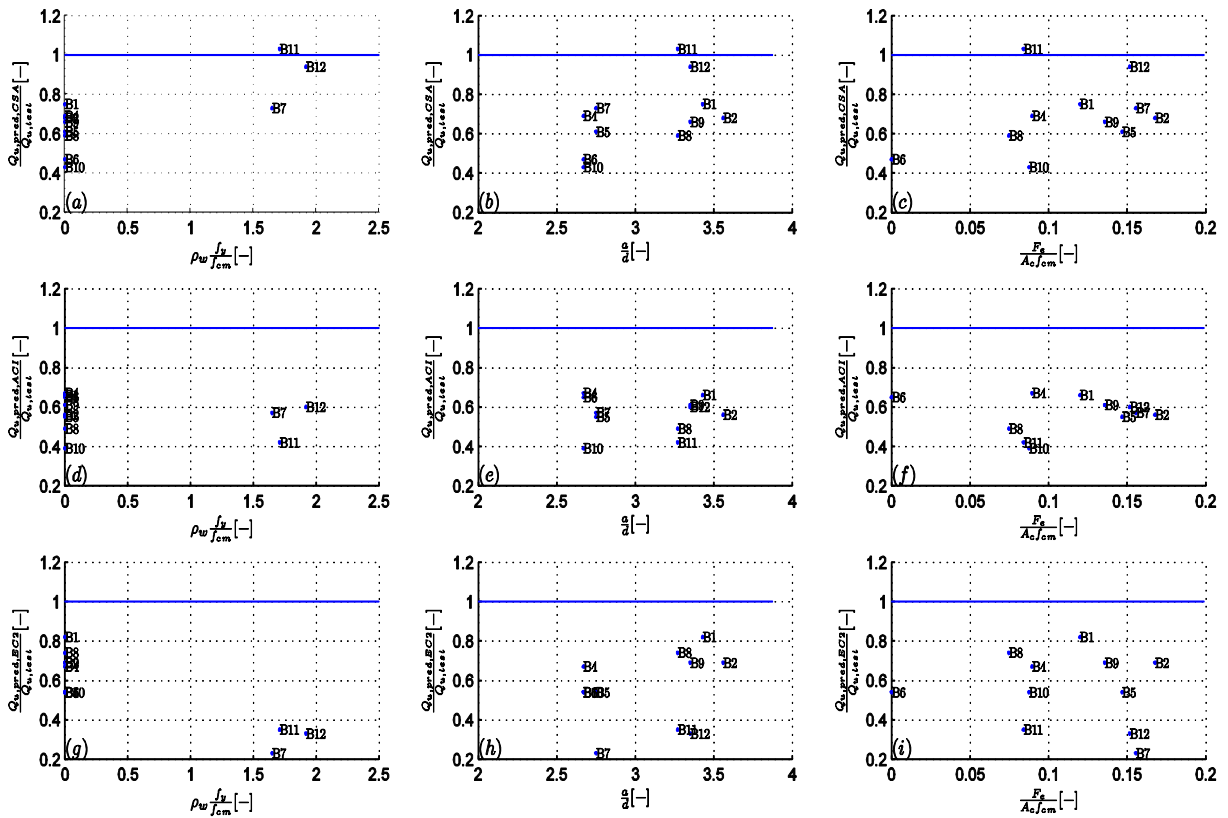


Fig. 5 Parameter analysis

CRACK PATTERN

In Fig. 6, the crack patterns of the 11 considered test specimens are depicted. The dashed zones indicate the location where failure was initiated. For the beams that failed in bending, the evolution of the crack pattern is the same: first a vertical bending crack initiated in the zone with constant moment. When the load Q was increased, new cracks formed. In the zone

with constant shear force, the cracks were inclined and had the same height as the vertical cracks in between the loading points. Failure occurred in the zone between the loading points due to excessive compression in the concrete. Although all beams had a 1 m (3.3 ft.) cantilever, beams B6 and B10 failed due to the loss of anchorage. Two main reasons can be given: (1) the low inclination of the cracks leads to high tensile forces in the longitudinal reinforcement. (2) Circular tensile stresses will be induced in the concrete surrounding the longitudinal reinforcement with improved bonding. Cracks will occur when these circular tensile stresses reach the concrete tensile strength making the transfer of bond stresses less effective.

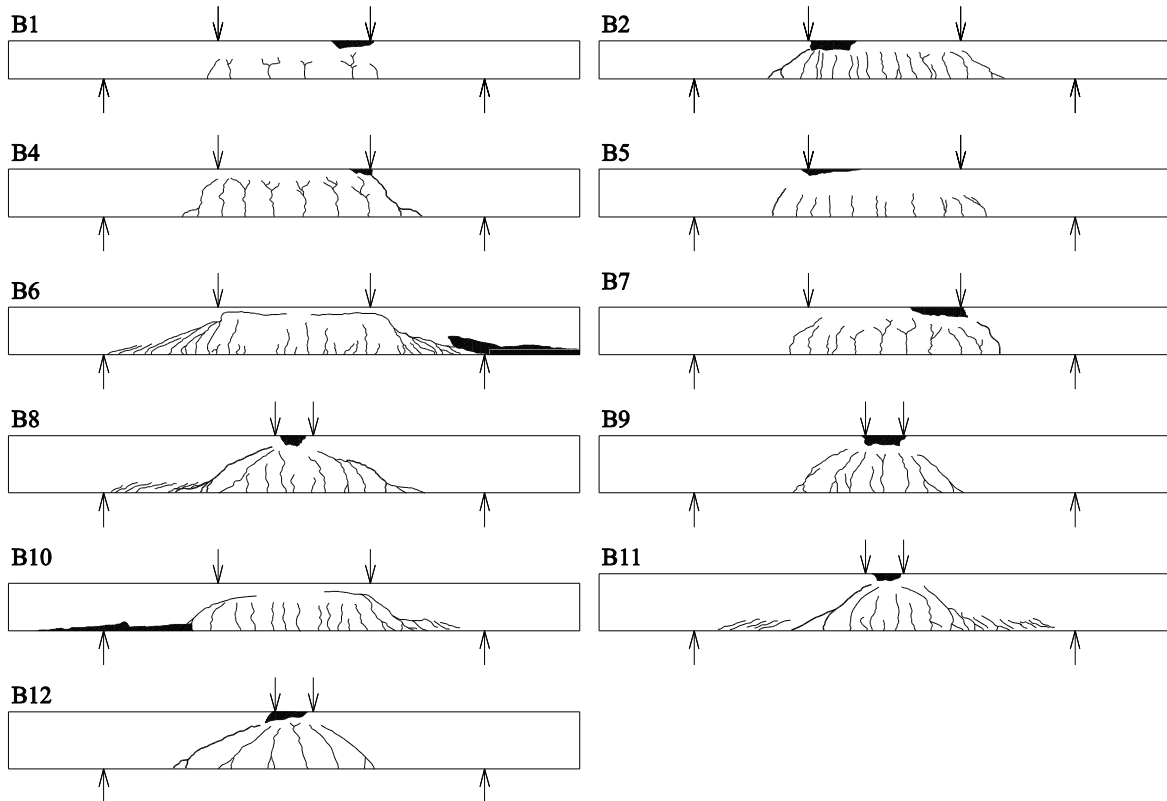


Fig. 6 Crack pattern at failure

Beams B1, B4 and B7 exhibited bifurcated cracks. These cracks started as normal vertical bending cracks. At high loads Q they started to bifurcate and tend to grow towards each other. A similar crack pattern was observed by Minelli²⁴ in his research on reinforced shear critical beams without stirrups having shear span to depth ratios equal to 2.5. The NSC0 set of beams consisted of 4 specimens, constructed with normal strength concrete and having comparable geometric properties as the beams described from the aforementioned experimental campaign. All specimens had 2 bars with a diameter of 24 mm (0.95 in.). The overall span and effective depth were equal to 4350 mm (14.3 ft.) respectively 435 mm (17.1 in.). Two specimens were loaded with a uniformly distributed load and two with two concentrated point loads. Two beams were equipped with bonded longitudinal reinforcement

whereas the other two specimens had a smooth plastic tube over the reinforcement to prevent bond between reinforcement and concrete. Fig. 7(a) and (b) show the crack pattern for the beams with bonded reinforcement at failure. Fig. 7(c) and (d) depict the crack pattern for the beams with unbonded reinforcement at failure.

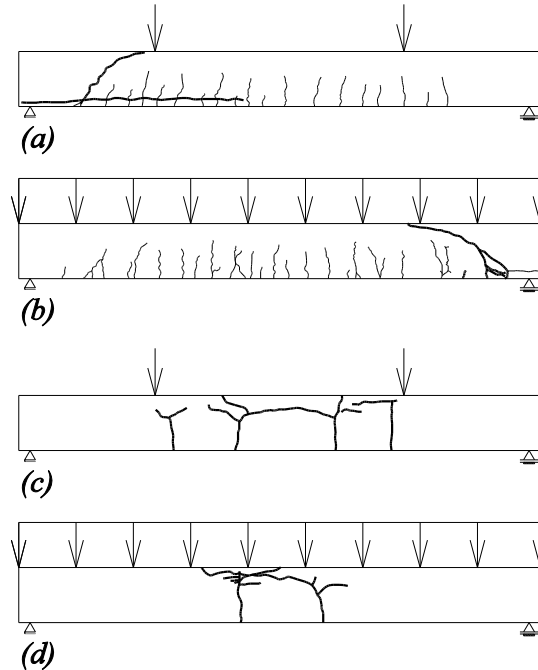


Fig. 7(a)-(d) Crack pattern at failure, adopted from Minelli²⁴

The two beams with unbonded reinforcement show a similar bifurcated crack pattern whereas the two specimens with bonded reinforcement failed due to the combined working of shear and flexure. When a beam is cracked, the external applied bending moment is resisted by the internal couple C (concrete compressive force) and T (reinforcement tensile force) with a lever arm equal to z ; i.e. $M = T z = Cz$. When this relationship is combined with the well-known relationship between shear and the rate of change of bending moment along the span, $V = dM/dx$, the shear is expressed as a combination of two components

$$V = z \frac{dT}{dx} + T \frac{dz}{dx} \quad (39)$$

The first term in Eq. (39) denotes the ‘beam’ action whereas the second term denotes the ‘arching’ action. If unbonded reinforcement is used, dT/dx equals zero and only arching action remains. This arch splits from the rest of the web resulting in bifurcated cracks. Arching action however, is generally believed to be only significant when the shear span to depth ratio is less than or equal to 2.5 (deep members)²⁵⁻²⁶. In those members, forces applied at the top are more likely to be transferred to the support by means of direct struts. For members with higher a/d -ratios, flexural action will be dominant. In order to avoid conservative results, Collins and Mitchell²⁵ propose the use of strut-and-tie models for deep

members and a sectional approach for more slender members. The shear carried by the arching mechanism could explain the discrepancy between the analytical predictions and the experimental observations.

ALTERNATIVE STRENGTH PREDICTION MODEL BASED ON ARCH ACTION

Although all beams in this experimental program had shear span to depth ratios between 2.6 and 3.6, an investigation can be made based on the aforementioned arching action. A considerable number of truss models that incorporate the arching mechanism for members with shear reinforcement are already presented in the literature²⁷⁻²⁹. An important point of discussion is the shape of the arching mechanism. Some researchers such as Kim and Jeong³⁰ propose a simple power law for the path of the compression force as a function of the coefficient α . This coefficient is equal to the ratio of shear carried by the arch to the total amount of shear. If α is equal to 1, the arching mechanism will take the form of a straight strut. Muttoni and Fernández Ruiz³¹ propose a straight strut in combination with an elbow shaped strut. The latter will be activated when the web of the beam in the shear zone is severely cracked.

From Fig. 6 it can be seen that all beams were nearly uncracked in the zone where a direct strut could be formed. All 11 beams are idealized as shown in Fig. 8(a). The remaining bearing system consists thus of two inclined struts, one horizontal strut and one horizontal tension tie at the center of the longitudinal reinforcement. If a prestressing force is applied, it is considered as an external applied load and it is converted to an equivalent system of horizontal nodal forces (P_1, P_2), depicted in Fig. 8(b). Both forces can be calculated by considering rotational and horizontal equivalency as also proposed by Ramirez³²

$$P_1 \left(d_p - \frac{c}{2} \right) = M_p + F_e \left(y_t - \frac{c}{2} \right) \quad (40)$$

$$P_2 = F_e - P_1 \quad (41)$$

where d_p is the center of the prestressing reinforcement, c is the height of the compression zone, y_t equals the distance from the top fiber to the neutral axis in uncracked state and M_p is the bending moment of the prestressing force around the neutral axis. The internal forces can be easily determined by considering the equilibrium of nodes [1] and [2] shown in Fig. 8(c). These forces are then given by

$$F_2 = \frac{Q}{\sin \theta} \quad (42)$$

$$F_1 = P_2 + Q \cot \theta \quad (43)$$

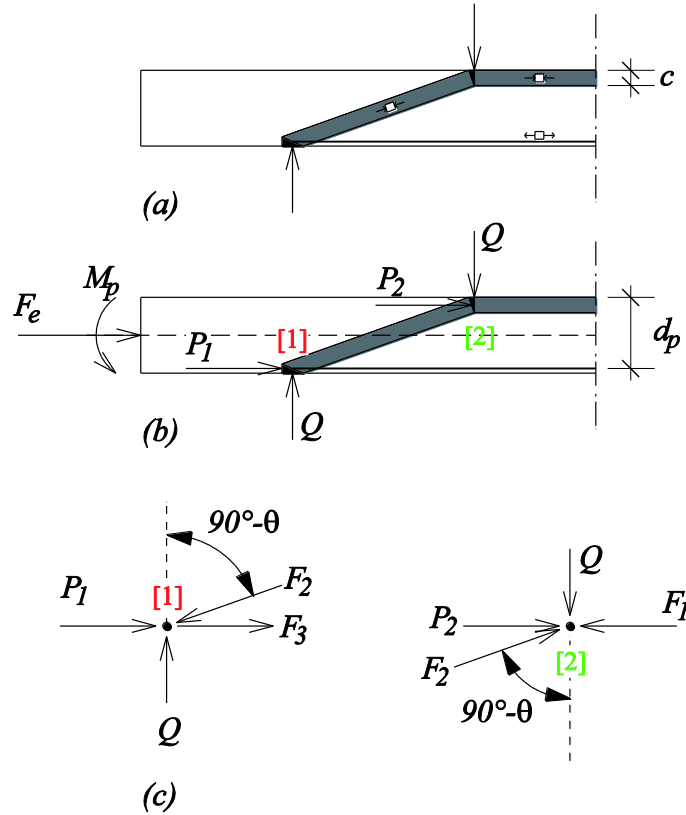


Fig. 8 Structural idealization

The height of the compression zone c can be determined from the equilibrium equations (44) and (45) of an elementary section (Fig. 9(a)) taken in between the two loading points. In the calculation, the hypothesis of Bernoulli is assumed to be valid between the loading points and the contribution of concrete in tension is neglected.

$$A_p' \sigma_p' + A_p \sigma_p + A_s \sigma_s = b \int_0^x \sigma_c(z) dz \quad (44)$$

$$M_{Ed} = bx_G \int_0^x \sigma_c(z) dz + A_s \sigma_s (d_s - x) + A_p \sigma_p (d_p - x) - A_p' \sigma_p' (x - d_p') \quad (45)$$

Fig. 9(b) depicts the nonlinear stress-strain relationship for concrete in compression, adopted from EC2¹¹. The analytical expression is given by Eq. (46) and is based on the work of Sargin and Handa³³.

$$\frac{\sigma_c}{f_{cm}} = \frac{k\eta - \eta^2}{1 + (k-2)\eta} \quad (46)$$

In Eq. (46), k denotes the plasticity number and is given by Eq. (47).

$$k = 1.05 E_c \frac{\varepsilon_{c1}}{f_{cm}} \quad (47)$$

The modulus of elasticity is taken equal to 38 GPa (5511 ksi) whereas the peak compressive strain ε_{c1} is assumed to be equal to 0.0035. The factor η denotes the ratio of the compressive strain ε_c to the peak compressive strain. Fig. 9(c) and 9(d) depict the standard bilinear stress-strain diagram for prestressing and conventional reinforcing steel respectively.

With the internal forces and geometry known, it is possible to calculate the stress in the components of the proposed bearing system. Failure will occur when either the compressive strength in the struts reaches the maximum compressive strength or when the tensile stress in the reinforcement reaches the ultimate tensile strength. No reduction on the strength of the compressive struts is used because these struts are not cracked due to shear. With the described geometry, it is possible to predict the bending failure mode. It is however not possible to predict the failure mode due to loss of anchorage. Table 5 lists the results from this procedure. All specimens are predicted to fail due to crushing of the horizontal strut. It can be seen that a good correlation can be found between the predicted failure load and the experimentally obtained strength. The average ratio between predicted and experimental failure load is equal to 0.94 with a COV of 4%.

Table 5 Predicted strengths obtained from proposed bearing system

Specimen	$Q_{u,test}$ kN (kip)	$Q_{u,pred}$ kN (kip)	$\frac{Q_{u,pred}}{Q_{u,test}}$
B1	196 (44)	176 (40)	0.90
B2	325 (73)	307 (69)	0.94
B4	259 (58)	232 (52)	0.90
B5	455 (102)	419 (94)	0.92
B6	222 (50)	214 (48)	0.96
B7	446 (100)	419 (94)	0.94
B8	318 (72)	333 (75)	1.05
B9	381 (86)	353 (79)	0.93
B10	413 (93)	394 (89)	0.95
B11	370 (83)	332 (75)	0.90

B12	385 (87)	353 (80)	0.92
μ			0.94
COV			4%

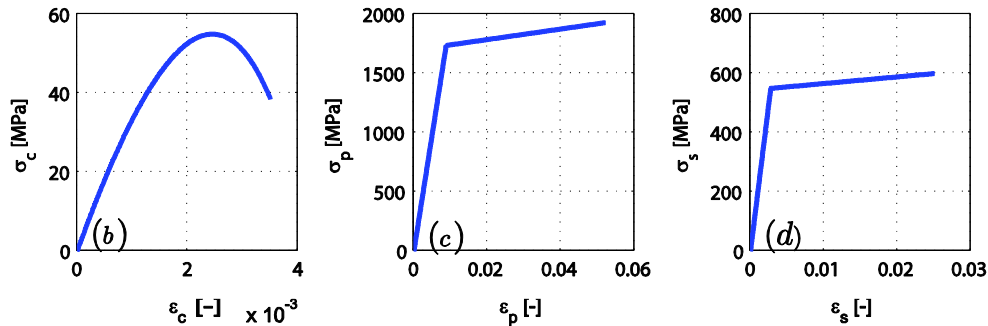
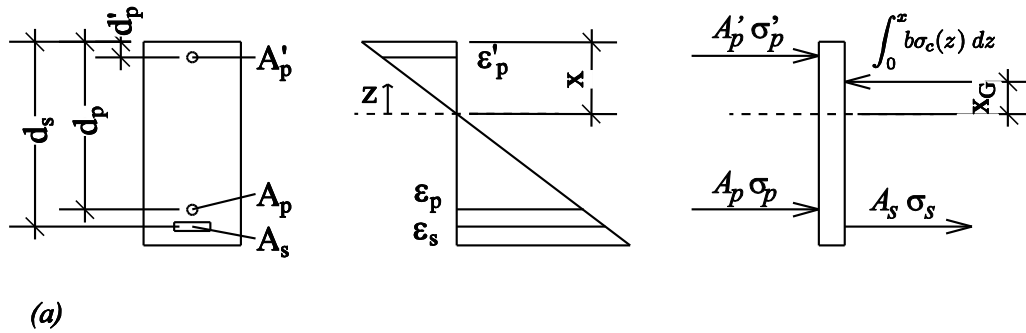


Fig. 9 (a) equilibrium conditions; (b) stress-strain relationship for concrete; (c) stress-strain relationship for prestressing steel; (d) stress-strain relationship for reinforcing steel (note: 1MPa = 145 psi)

SUMMARY AND CONCLUSIONS

In this paper an experimental program is presented consisting of 12 full scale rectangular (partially) prestressed and reinforced concrete beams. These specimens were subjected to a four-point bending test until failure occurred. The main investigated parameters were the amount of prestressing, amount of longitudinal and transverse reinforcement and effective depth respectively. The experimentally obtained results were compared to shear strength predictions according to the American, European and Canadian codes of practice.

It was found that all building codes severely underestimated the failure load even with all safety and strength reduction factors equal to 1. The average predicted-over-experimental failure load ratio was equal to 0.60 with a coefficient of variation of 26%.

A separate investigation was performed for each code of practice to determine the influence of the aforementioned parameters on the shear strength prediction. All three building codes showed the trend that decreasing shear span to depth ratios result in decreasing predicted-over-experimental failure loads. This is due to the fact that the members with the lowest shear span to depth ratio, around 2.6, are more likely to transfer vertical forces directly to the support via a strut and tie mechanism.

Concerning the influence of the amount of prestressing, the same pattern is observed for all considered codes of practice. An increase of the amount of prestressing results in an increase and decrease of the predicted-over-experimental failure load ratio. Based on the obtained test results, it seems that current codes of practice do not account for the positive effect of increasing amount of prestressing on the shear capacity.

Beams with shear reinforcement are better predicted by the Canadian code of practice than their equivalents without shear reinforcement. The opposite trend is observed for EC2 whereas the level of safety remains relatively the same when using ACI318-08.

A possible explanation for the discrepancy between predicted and experimental strengths could be the presence of the arching mechanism carrying all the shear force at failure.

NOTATION

A_g	= gross area of concrete section [mm ²]
A_{ps}	= area of prestressed longitudinal reinforcement on the flexural tension side [mm ²]
A_s	= area of longitudinal reinforcement [mm ²]
A_v	= area of shear reinforcement [mm ²]
A_{sv}	= area of shear reinforcement [mm ²]
b_w	= width of web [mm]
d	= effective depth [mm]
d_p	= distance from extreme compression fiber to center of prestressing reinforcement [mm]
d_v	= effective shear depth [mm], taken as the flexural lever arm but not less than $0.9d$
E_s	= elastic modulus of steel [N/mm ²]
E_c	= secans elastic modulus of concrete [N/mm ²]
f_c'	= specified concrete compression strength [N/mm ²]
f_{ck}	= characteristic concrete compression strength [N/mm ²]
f_{cd}	= design concrete compression strength [N/mm ²]
f_{p0}	= stress in the tendon when the surrounding concrete is at zero stress, wich may be taken as 1.1 times the effective stress in the prestressing tendons f_{se} after all lossen [N/mm ²]
f_{pc}	= compressive stress at center of concrete cross section after allowance of all prestress losses and resisting externally applied loads [N/mm ²]
f_y	= specified yield strength of steel [N/mm ²]
f_{yt}	= specified yield strength of transverse reinforcement [N/mm ²]
f_{ywd}	= design yield strength of transverse reinforcement [N/mm ²]

- k = size effect factor equal to $1+(200/d)^{0.5}$, with d expressed in [mm]
 M_{cre} = moment causing flexural cracking due to externally applied loads [Nmm]
 M_{max} = maximum factored moment at section due to externally applied loads [Nmm]
 M_u = factored moment at section [Nmm]
 N_u = factored axial force, occurring simultaneously with V_u or T_u [N]
 T_u = factored torsional moment [Nmm]
 s = center-to-center spacing of shear reinforcement [mm]
 V_c = concrete contribution [N]
 V_{ci} = nominal shear strength provided by concrete when diagonal cracking results from combined shear and moment [N]
 V_{cw} = nominal shear strength provided by concrete when diagonal cracking results from high principal tensile stress in web [N]
 V_d = shear force at section due to unfactored dead load [N]
 V_i = factored shear force at section occurring simultaneously with M_{max} [N]
 v_{min} = $0.035k^{3/2}f_{ck}^{1/2}$ [N/mm²]
 V_n = nominal shear strength [N]
 V_p = vertical component of the tensile force in the prestressing tendons [N]
 V_r = resisting shear strength [N]
 $V_{r,max}$ = shear force needed to cause crushing of the inclined struts, equal to $0.25\phi_p f_c 'b_w d_v + V_p$ [N]
 V_{Rd} = design resisting shear strength [N]
 $V_{Rd,c}$ = design shear resistance provided by concrete [N]
 $V_{Rd,s}$ = design shear resistance provided by shear reinforcement [N]
 $V_{Rd,max}$ = design ultimate shear resistance to web compression [N]
 V_s = contribution of shear reinforcement to total shear strength [N]
 V_u = factored shear force at section [N]
 z = internal lever arm, can be taken as $0.9d$ [mm]
 α = angle of shear reinforcement [$^\circ$]
 β = concrete tensile stress factor indicating the ability of diagonally cracked concrete to resist shear
 γ_c = safety factor for concrete
 θ = angle between compression field and tension chord [$^\circ$]
 ρ_l = ratio of A_s to $b_w d$
 ρ_w = ratio of A_s to $b_w d$
 σ_{cp} = average concrete compressive stress due to prestressing force [N/mm²]
 ϕ_p = strength reduction factor for prestressing steel, in the presented calculations taken equal to 1.

REFERENCES

1. Ritter, W., “Die Bauweise Hennebique”, *Schweizerische Bauzeitung*, February 1899, 41-61
2. Mörsch, E., “Der Eisenbetonbau – Seine Theorie und Anwendung”, *Verlag von Konrad Wittwer*, V.1 Part 1, 1920, Stuttgart
3. Mörsch, E., “Der Eisenbetonbau – Seine Theorie und Anwendung”, *Verlag von Konrad Wittwer*, V.1 Part 2, 1922, Stuttgart
4. Withey, M. O., “Tests of Plain and Reinforced Concrete Series of 1906”, *Bulletin of the University of Wisconsin, Engineering Series*, V.4, No. 1, 1907, 1-66
5. Talbot, A. N., “Tests of Reinforced Concrete Beams: Resistance to Web Stresses Series of 1907”, *Bulletin 29*, University of Illinois Engineering Experiment Station, Urbana, Ill. 1909
6. ACI-ASCE Committee 445 on Shear and Torsion, “Recent Approaches to Shear Design of Structural Concrete”, *Journal of Structural Engineering*, V.124, No. 12, December 1998, 1375-1417
7. Kupfer, H., “Erweiterung der Mörsch schen Fachwerkanalogie mit Hilfe des Prinzips vom Minimum der Formänderungsarbeit”, *Comité Euro-International du Béton, Bulletin d’Information*, No. 40, 1964, CEB, Paris, 44-57
8. Caflisch, R., Krauss, R., Thurlimann, B., “Biege- und Schub-versuche an teilweise vorgespannten Betonbalken”, *Serie C., Bericht 6504-3*, 1971, Institut für Baustatik, ETH, Zürich
9. Lampert, P., Thurlimann, B., “Ultimate Strength and Design of Reinforced Concrete Beams in Torsion and Bending”, *IABSE*, No. 31-I, 1971, pp. 107-131
10. Thurlimann, B., Marti, P., Pralong, J., Ritz, P., Zimmerli, B., “Vorlesung Zum Bortbildungskurs für Bauingenieure”, 1983, Institut für Bautechnik und Konstruktion, ETH, Zürich
11. Comité Euro-International du Béton (CEB), “Shear and Torsion, June: Explanatory and Viewpoint Papers on Model Code Chapter 11 and 12, prepared by CEB Committee V”, *CEB Bulletin*, No. 12, 1978, CEB, Paris
12. Ramirez, J. A., “Evaluation of a Modified Truss-Model Approach for Beams in Shear”, *ACI Structural Journal*, V.88, No. 5, 1991, pp. 562-571
13. ACI Committee 318, “Building Code Requirements for Reinforced Concrete (ACI 318M-08) and Commentary”, 2008, American Concrete Institute, Farmington Hills, Michigan
14. European Committee for Standardization, “Eurocode 2. Design of Concrete Structures – Part 1-1: General Rules and Rules for Buildings”, 2004, CEN, Lausanne
15. European Committee for Standardization, “Eurocode 2. Design of Concrete Structures – Part 1-1: General Rules and Rules for Buildings: National Application Document”, 2010, NBN, Brussels
16. Baumann, T., “Zur Frage der Netzbewehrung von Flächen trag-werken”, *Bauingenieur*, V. 47, No. 10, 1972, 367-377
17. Collins, M. P., “Towards a Rational Theory for RC Members in Shear”, *Journal of the Structural Division*, V. 104, No. 4, 1978, 649-666

18. Vecchio, F. J., Collins M. P., “The Modified Compression-Field Theory for Reinforced Concrete Elements Subjected to Shear”, *ACI Structural Journal*, V. 83, No. 2, 1983, 219-231
19. Bhide, S. B., Collins, M. P., “Influence of Axial Tension on the Shear Capacity of Reinforced Concrete Members”, *ACI Structural Journal*, V. 86, No. 5, 1989, 570-581
20. Walraven, J. C., “Fundamental Analysis of Aggregate Interlock”, *Journal of the Structural Division*, V. 107, No. 11, 1981, 2245-2270
21. Wong, P. S., Vecchio, F. J., “VecTor 2 & FormWorks Users’s Manual”, Department of Civil Engineering, University of Toronto, Toronto, Ontario, 2002
22. Bentz, E. C., “Sectional Analysis of Reinforced Concrete Members”, PhD Thesis, Department of Civil Engineering, University of Toronto, Toronto, Ontario, 2000
23. CSA Committee A.23.3, “Design of Concrete Structures (CSA A.23.3-04), Canadian Standards Association, Mississauga, 2004
24. Minelli, F., Plain and Fiber Reinforced Concrete Beams under Shear Loading: Structural Behavior and Design Aspects”, PhD Thesis, Department of Civil, Architectural, Environmental and Land Planning, University of Brescia, Brescia, 2005
25. Collins, M. P., Mitchell, D., “Prestressed Concrete Structures”, Prentice Hall, Englewood Cliffs, N.J., 1991
26. Park, H. G., Choi, K. K., Wight, J. K., “Strain-Based Shear Strength Model for Slender Beams without Web Reinforcement”, *ACI Structural Journal*, V. 103, No. 6, 2006, 783-793
27. Marti, P., “Basic Tools of Reinforced Concrete Beam Design”, *ACI Structural Journal*, V. 82, No. 1, 1985, 46-56
28. Walraven, J. C., Lehwalter, N., “Size Effect in Short Beams Loaded in Shear”, *ACI Structural Journal*, V. 91, No. 5, 1994, 585-593
29. Leonhardt, F., “Reducing the Shear Reinforcement in Reinforced Concrete Beams and Slabs”, *Magazine of Concrete Research*, V. 17, No. 53, 1965, 187-198
30. Kim, W., Jeong, J., “Decoupling of Arch Action in Shear-Critical Reinforced Concrete Beams”, *ACI Structural Journal*, V. 108, No.4, 2011, 395-404
31. Muttoni, A., Fernández Ruiz, M., “Shear Strength of Members without Transverse Reinforcement as Function of Critical Shear Crack Width”, *ACI Structural Journal*, V. 105, No. 2, 2008, 163-172
32. Ramirez, J. A., “Strut-Tie Design of Pretensioned Concrete Members”, *ACI Structural Journal*, V. 91, No. 4, 1994, 572-578
33. Sargin, M., Handa, V., “A General Formulation for the Stress-Strain Properties of Concrete,” *Report no. 3*, 1969, University of Waterloo